[Invited] Near-Infrared Sensitivity Improvement by Plasmonic Diffraction Technology

Nobukazu Teranishi and Atsushi Ono
Research Institute of Electronics, Shizuoka University
3-5-1 Johoku, Hamamatsu, 432-8011 Japan
E-mail: teranishi@idl.rie.shizuoka.ac.jp

Abstract Plasmonic diffraction technology for silicon image sensor is reviewd, which increases near-infrared (NIR) sensitivity. To overcome the poor NIR absorption in silicon without the silicon thickness increase, the metal grating is formed on the entrance surface. At the quasi-resonant condition, the reflectance is still small, and the incident light is emitted into the silicon with large diffraction angle. The diffracted light travels back and forth between high reflective DTIs (deep trench isolation). The effective light trace (*ELT*) is extended by the light confinement in a pixel. Ag, Cu and Al is suitable for DTI material for high reflectance and DTI width shrinkage. The resonant chamber effect is shown, which enhances the absorptance. In simulation, absorptance in 3.25 μm-thick silicon was increase to 47 % by these technologies.

To enhance specific

Keywords: image sensor**,** plasmonic diffraction, near-infrared, deep trench isolation, resonant chamber effect

1. Introduction

Plasmonic diffraction technology for near-infrared (NIR) sensitivity improvement are explained, based on these papers [1-5]. This method's target applications are ToF (time of flight), night monitoring, biometrics. Laser or LED (light emitted diode) of 940 nm or 850 nm wavelength are usually applied for illumination (Slide 4, 5). For automobile application, 940 nm is mainly used because human eye cannot detect it, and the sunlight power is rather small. However, there still exists a large background of the sunlight. Therefore, it is preferable that sensitivity increases only for specific wavelength. Then, background light influence is suppressed to some extent.

However, there is a serious problem for NIR imaging, which is the poor sensitivity due to the poor absorption in silicon (Slide 6) [6]. When the wavelength becomes longer, the absorption becomes drastically smaller. The Si absorption coefficient at 940 nm wavelength is 2-decade smaller than that of 450 nm and is 1-decade smaller than that of 700 nm. To realize 50 % absorptance, 38 um Si thickness is needed for 940 nm. Although the absorption becomes improved if the Si thickness is increased, there are difficulties; one is deep and narrow DTI (deep trench isolation) process. Another is epitaxial defects. Thirdly, even if deep photodiode dopant profile is optimized using high energy ion implantation, the vertical electric field remains small (Slide 7).

To increase Si absorption without Si thickness increase, the approaches which increases effective light trace (*ELT*) were proposed (Slide 8). The incident light is bent by various methods at the entrance of the silicon, refraction by pyramid array [7, 8], scattered by scatterer [9,10], and diffraction by poly-Si grating [11]. The bent light is reflected on the DTI. Then, the *ELT* is increased and the absorptance is also increased. As a result, NIR sensitivity is enhanced.

2. Plasmonic diffraction under quasi-resonant condition

We proposed plasmonic dffraction under quasi-resonant condition [1-5]. metal grating is located on the entrance surface of BSI image sensor, as shown in Slide 10. At the resonant condition, the reflectance becomes minimum, and the incident light is diffracted at 90 degree. At the quasi-resonant condition, the reflectance is still small, and the incident light is diffracted nearby 90 degree and is emitted into the Si. High reflective DTI, using Ag, Cu and Al, is also recommended for light confinement.

The diffraction angle is determined by the equation, as shown in Slide 11. l is diffraction order, n_{Si} is the real part of refractive index for Si, p is grating period. Two cases were studied; One is Case I, which includes only 1st-order diffraction. The other is Case II, which includes 1st-order and 2nd-order diffractions. The figures in Slide 11 are electric field intensity distributions after optimizing the grating dimensions by maximization of the absorptance. Although the spaces of the grating were much smaller than the wavelength in both cases, normal incident light was diffracted and was conducted into Si.

The table in Slide 12 compares between Case I and Case II. The optimized Ag grating dimensions are obtained for 6.5 um pixel size. In Case I, the space is only 35 nm, which is small for backside process. In Case II, the space becomes 150 nm, which is sufficiently large. Eventually, both Case I and Case II showed good Si absorptance. However, Case II has disadvantage for pixel shrinkage because several grating lines might be needed in a pixel.

Electric field distribution, Si absorption, Ag grating absorption, Ag DTI absorptiion, reflectance etc. are calculated using FDTD (Slide 13). Ag is selected as grating and DTI metal because Ag has the lowest absorption loss around 940 nm. DTI width is 180 nm, and the protection SiO_2 covers Ag grating. PML, perfectly matched layer, surrounds the pixel.

The electric field intensity distributions for Case I and Case II were obtained, as shown in Slide 14. Normal incident light was diffracted to theoretically 81 degree in Case I and 85 degree and 30 degree in Case II. 0th-order diffraction seemed small. In enlarged figures, electric multipoles were seen in the Ag grating, and they generated diffracted light toward Si. The light consumption ratios are shown in Slide 15. Both showed large diffraction efficiencies, 50 % and 46 % and low reflectance 7 % and 2 %, respectively. Therefore, both cases have sufficient potential for NIR absorption improvement.

3. Requirement for DTI

Next, the necessity of high reflective DTI is explained. DTI between pixels reduces both electron-diffusion crosstalk and optical crosstalk. It also contributes to the Si absorption increase by light confinement. However, DTI does not directly contribute to sensitivity. Therefore, the shrinkage of DTI is required. Hereafter, the requirements for DTI are studied [1,5].

As seen in Slide 17, the bent light is reflected by DTI with a loss of 1-*R*. *R* is the reflectance of Si/DTI interface. *ELT* becomes a geometric series and is proportional to this equation. *k* is the number of reflections. The right figure shows the *ELT* dependence on reflectance for various *k*. When reflectance is smaller than 0.8, *ELT* does not increase even if *k* increases. When reflectance is larger than 0.8, *ELT* rapidly increases with *k*. Therefore, it is preferable that reflectance is larger than 0.8.

Reflectance contours of normal incident to DTI for combination of n_{DTI} and k_{DTI} is shown in Slide 18. The reflectance for normal incidence is given by this formula. n_{Si} and k_{Si} are real part and imaginary part of the refractive index of Si. n_{DTI} and k_{DTI} are those for the DTI material. The horizontal axis indicates n_{DTI}, while the vertical axis indicates k_{DTI}. Wavelengths are 1100nm and 800 nm. There is little difference between them. When k_{DTI} increases and n_{DTI} decreases, reflectance increases, as indicated by the red arrow. The green circles point various materials' indexes at 940 nm wavelength. Ag, Cu, Au, and Bi achieve more than 0.9 reflectance. Al has 0.76 reflectance.

To compare SiO_2 DTI with metal-filled DTI, incident angle dependence of reflectance is shown for various DTI width in Slide 19. SiO_2 DTI has low reflectance below the critical angle. Even over the critical angle, the reflectance is significantly reduced as DTI width decreases because of evanescent light penetration. Various angle light is generated in the pixel because the pixel shape is not simple. The vertical transfer gate is an extreme case. Therefore, SiO_2 DTI is not suitable for both optical crosstalk suppression and light confinement. In contrast, Ag and Cu constantly keep high reflectance for all incident angle.

Slide 20 shows DTI width dependence of reflectance and transmittance. Dashed line indicates the case where 5nm-thick Al_2O_3 layer exists between Si and DTI material. Real line indicates the case without Al_2O_3. Thin Al_2O_3 layer can be neglected from optical perspective. Reflectance decreases below 50 nm width even for metal filled DTI. To maintain more-than-90 % reflectance, Ag width of 38 nm and Cu width of 53 nm are required. 40 nm width is needed for Al to keep more than 75 % reflectance. Transmittance exponentially decreases as the width increases. To maintain less-than-5 % transmittance, DTI width of 35 nm for Al, 50 nm for Ag, and 55 nm for Cu are required. DTI width shrinkage is limited even for metal DTI. Still, Ag, Cu, and Al are suitable for high reflective DTI.

4. Resonant-chamber-like pixel

In this section, concept of resonant-chamber-like pixel is introduced.

More realistic situation was simulated, which has PMD SiO_2 under Si and Cu reflector (Slide 22). The Si thickness is 3 μm in Case I, and 3.25 μm in Case II. PMD SiO_2 thickness is 800 nm. The first Cu wiring layer is applied for the reflector. Slide 23 shows the simulation results for Case I. The absorptance in Si is increased from 7 % to 31 % when Ag grating is attached. Resonant patterns are clearly seen in both x and z directions. However, bad news is that large reflection is still observed due to the decoupling of the reverse light. Propagation angle, θ, is calculated from the number of anti-nodes, m_x and m_z, by this formula (Slide 24). Here, k_x and k_z are wave numbers, and l_x and l_z are the size of Si. The obtained θ is 80 degree, which has a good agreement with theoretical diffraction angle , 80.6 degree. Therefore, the incident light was really diffracted to 80 deg. and was propagated at 80 degree. Slide 25 explains the mechanism of the decoupled light generation. The diffracted light travels in Si, reflecting on DTI. Then, the light is total-reflected on the Si/SiO_2 interface at the bottom and propagates at the reverse pass. The reverse light has the same angle as the diffraction angle θ_d. Decoupled light is generated by surface plasmon resonance at the metal grating. Therefore, large reflection is still observed.

Slide 26 shows Case II results. The resonant patterns are not so clear because there are both 1st-order and 2nd-order diffractions. However, the numbers of anti-nodes can be counted. The absorptance in Si is also much increased to 47 %, which is better than that of Case I. Reflectance of Case II is much smaller than that of Case I. Larger absorptance and smaller reflectance are because the electric field distribution is more complicated, and the decoupling at the grating might be smaller.

The graph in Slide 27 shows DTI span dependence of absorptance for Case I. There is no bottom SiO_2 and Cu reflector in this simulation. Therefore, resonance occurs only in x direction. Absorptance sinusoidally oscillates with a period of 268 nm of DTI span. The period is nearly equal to the wavelength in Si. Resonant pattern is clearer when the absorptance is larger. The graph in Slide 28 shows Si thickness, l_z, dependence of absorptance and reflectance. Absorptance and reflectance periodically oscillate with Si thickness. When Si thickness is 3.25 um, absorptance exhibits a peak, and the resonant pattern is clearer. On the other hand, when Si thickness is 3 um, absorptance exhibits a dip, and the resonant pattern is not clear. Anti-node number in z-direction for each peak is incremented by one. According to these results, resonant chamber effect affects absorptance. To achieve resonant chamber condition, diffraction angle, θ_d, should be optimized for each pixel size by tuning the grating period.

5. Conclusions

To enhance specific wavelength sensitivity, we proposed plasmonic diffraction technology, which achieves large diffraction angle and large diffraction efficiency. High reflective DTI is indispensable for light confinement in the pixel. Cu, and Al are preferable for high reflective DTI. Although they are advantageous for DTI width shrinkage compared with other material, there exists limitation of

DTI width shrinkage from the optical aspect. The metal grating, high reflective DTI and the bottom reflection can make a resonant chamber. The resonant state enhances the absorption in Si.

In simulation, absorptance in 3 μm-thick-Si was increased from 7 % to 31 % in Case I. In Case II, 47 % absorptance is obtained in 3.25 μm-thick Si.

Acknowledgment

This research was partially supported by NICT commissioned research (03601) and JSPS KAKENHI (JP22K18984).

References

[1] A. Ono, K. Hashimoto, N. Teranishi, “Near-infrared sensitivity improvement by plasmonic diffraction for a silicon image sensor with deep trench isolation filled with highly reflective metal”, Opt. Express, vol. 4, pp. 960-968, 2021.

[2] “Plasmonic diffraction for the sensitivity enhancement of silicon image sensor”, International Image Sensors Workshop, P11, pp.138-141, Web-meeting, September 21, 2021.

[3] T. Yoshinaga, K. Hashimoto, N. Teranishi, Atsushi Ono, “Photon Confinement in a Silicon Cavity of an Image Sensor by Plasmonic Diffraction for Near-Infrared Absorption Enhancement”, Optics Express, vol.30, no.20, pp.35516-35525, 2022,

[4] T. Yoshinaga, K. Hashimoto, N. Teranishi, A. Ono, “Near-Infrared Sensitivity Enhancement of Silicon Image Sensor by Photon Confinement with Plasmonic Diffraction”, Int. Conf. on Solid State Devices and Materials (SSDM), G-5-05, Chiba, September 28, 2022.

[5] N. Teranishi, T. Yoshinaga, K. Hashimoto, A. Ono, “Near-Infrared Sensitivity Enhancement by 2^{nd}-Order Plasmonic Diffraction and Resonant-Chamber-Like Pixel,” IEEE IEDM, 37.2, San Francisco, USA, December 7, 2022.

[6] M. A. Green, “Self-consistent optical parameters of intrinsic silicon at 300 K including temperature coefficients”, Solar Energy Materials & Solar Cells, vol.92, pp.1305-1310, 2008.

[7] S. Yokogawa, I. Oshiyama, H. Ikeda, Y. Ebiko, T. Hirano, S. Saito, T. Oinoue, Y. Hagimoto, and H. Iwamoto, “IR sensitivity enhancement of CMOS image sensor with diffractive light trapping pixels”, Sci. Rep., vol. 7, pp.960-968, 2017.

[8] K. Zang, X. Jiang, Y. Huo, X. Ding, M. Morea, X. Chen, C. Chen, C-Y. Lu, J. Ma, M. Zhou, Z. Xia,Z. Yu, T. I. Kamins, Q. Zhang, J. S. Harris, “Silicon single-photon avalanche diodes with nano-structured light trapping”, *Nature communications*, *8*(1), 1-6, 2017.

[9] J. Park, Y. Lee, B. Kim, B. Kim, J. Park, E. Yeom, Y. Jung, T. Kim, H. Yoon, Y. Kim, J. Park, C-R. Moon, and Y. Park, “Pixel Technology for Improving IR Quantum Efficiency of Backside-illuminated CMOS Image Sensor”, IISW, R14, Snowbird, USA, 2019.

[10] E. P. Devine, W. Qarony, A. ahamed, A. S. Mayet, S. Ghandiparsi, C. Bartolo-Perez, A. F. Elrefaie, T. Yamada, S-Y. Wang, M. S. islam, “Single microhole per pixel in CMOS image sensor with enhanced optical sensitivity in near-infrared”, IEEE Sensors Journal, vol.21, no. 9, pp.10566-10562, 2021.

[11] E. Cobo, S. Massenot, A. L. Roch, F. Corbiere, V. Goiffon, P. Magnan, and J.-L. Pelouard, “Design of a CMOS image sensor pixel with embedded polysilicon nano-grating for near-infrared imaging enhancement”, Applied Optics, vol. 61,no. 4, pp.960-968, 2022.

5th International Workshop on Image Sensors and imaging Systems (2022 IWISS)
December 13,2022

Near-Infrared Sensitivity Improvement by Plasmonic Diffraction Technology

Nobukazu Teranishi and Atsushi Ono

Shizuoka University

References of Our Work

2

A. Ono, K. Hashimoto, N. Teranishi,
"Near-infrared sensitivity improvement by plasmonic diffraction for a silicon image sensor with deep trench isolation filled with highly reflective metal",
Opt. Express, vol. 4, pp. 960-968, 2021.

A. Ono, K. Hashimoto, T. Yoshinaga, N. Teranishi,
"Plasmonic diffraction for the sensitivity enhancement of silicon image sensor",
International Image Sensors Workshop, P11, pp.138-141, Web-meeting, September 21, 2021.

T. Yoshinaga, K. Hashimoto, N. Teranishi, Atsushi Ono,
"Photon Confinement in a Silicon Cavity of an Image Sensor by Plasmonic Diffraction for Near-Infrared Absorption Enhancement",
Optics Express, vol 30, no 20, pp 35516-35525, 2022,

T. Yoshinaga, K. Hashimoto, N. Teranishi, A. Ono,
"Near-Infrared Sensitivity Enhancement of Silicon Image Sensor by Photon Confinement with Plasmonic Diffraction",
Int. Conf. on Solid State Devices and Materials (SSDM), G-5-05, Chiba, September 28, 2022.

N. Teranishi, T. Yoshinaga, K. Hashimoto, A. Ono, "Near-Infrared Sensitivity Enhancement by 2nd-Order Plasmonic Diffraction and Resonant-Chamber-Like Pixel,"
IEEE IEDM, 37.2, San Francisco, USA, December 7, 2022.

Outline

3

Target Application Examples (1)

4

Time of Flight (ToF)

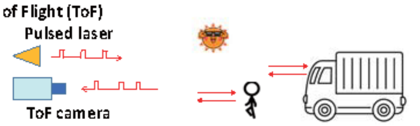

Situation
- Specific wavelength in NIR (940 nm, 850 nm)
- Polarized light by laser
  Usually remaining polarization when reflecting
- Large background light

Requirement
- Sensitivity increase only for specific wavelength and for polarization

Target Application Examples (2)

5

Night monitoring
- NIR camera + NIR illuminator
- Hospital, care
  Animal husbandry
  Security

MOWCAM (Trinity)
https://www.trinity4e.com/products/mowcam.html

Iris verification during walking

NEC, 6 Nov. 2019
https://jpn.nec.com/press/201911/20191106_01.html

NIR Absorption in Si

6

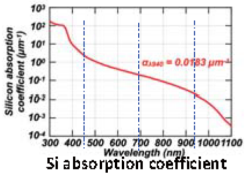

Si absorption coefficient
(M. A. Green et al., Solar Energy Materials & Solar Cells, 2008)

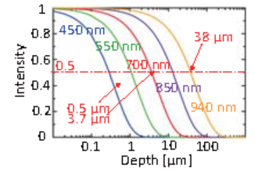

Light absorption in Si

- Poor NIR absorption in Si.
- Si thickness, which realizes 50 % absorptance,
  0.5 μm for 450 nm
  3.7 μm for 700 nm
  38 μm for 940 nm.

Difficulties of Thick Si Pixel

7

- Thick Si pixel can increase NIR absorption.
- There are difficulties to realize thick Si.
- NIR absorption increase technology without Si thickness increase is required.

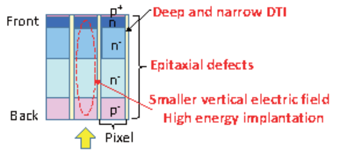

Sensitivity Increase by Effective Light Trace (ELT) Increase

8

Pyramid array
S. Yokogawa et al., Sci. Rep., 2017

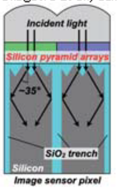

- Refracted by pyramid array
- Anisotropic etching
- Sensitivity (940 nm): x1.9

Scatterer (BST)
J-H. Park et al., IISW, 2019

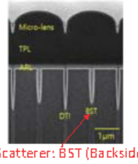

- Scattered by scatterer
- DTI like process
- Sensitivity (940 nm): x1.5

poly-Si grating
E. Cobo, Appl. Opt., 2022

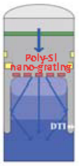

- Diffracted by ploy-Si grating
- Poly-Si gate process
- Sensitivity (850 nm): x1.33

Outline

Plasmonic Diffraction under Quasi-Resonant Condition

(A. Ono et al., Opt. Express, 2021, T. Yoshinaga et al., Opt. Express, 2022)

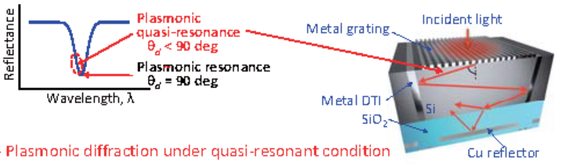

- Plasmonic diffraction under quasi-resonant condition
  => Low reflectance
  Large diffraction angle
- High reflective DTI, SiO_2 => Ag, Cu, Al
- Absorptance of 940 nm wavelength in Si was enhanced as 5〜6 times in simulation.

Diffraction Angle of Plasmonic Quasi-Resonant Condition

(A. Ono et al., Opt. Express, 2021, N. Teranishi et al., IEDM, 2022)

- Diffraction angle
  $\theta_d = \arcsin(l\lambda/n_{Si}p)$
  l: Diffraction order, λ: Wavelength
  n_{Si}: Refractive index for Si, p: grating period
- Case I includes only 1st-order diffraction
  Case II includes 1st-order and 2nd-order diffractions,

Case I
$\theta_d(1)$=81°

Case II
$\theta_d(1)$=30°
$\theta_d(2)$=85°

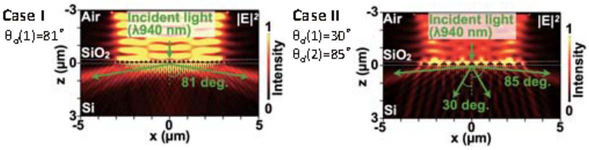

Comparison between Case I and Case II

	Case I	Case II
Diffraction order	1st-order	1st-order & 2nd-ordr
Optimized Ag grating dimension (nm)	p=265, w=230, s=35, h=85 (Si thickness: 3 μm)	p=525, w=375, s=150, h=90 (Si thickness: 3,25 μm)
Diffraction angle, $\theta_d(order)$	$\theta_d(1)$ = 81°	$\theta_d(1)$ = 30°, $\theta_d(2)$ = 85°
Fine pattern technology	Required	Not required
Pixel shrinkage	Advantage	Disadvantage

(Note: λ = 940 nm, pixel size = 6.5 μm)

- In Case I, grating space is only 35 nm, which is small for backside process.
  In Case II, grating space is 150 nm, which is sufficiently large.
- Case II has disadvantage for pixel shrinkage because several grating lines might be needed in a pixel.

Simulation Model

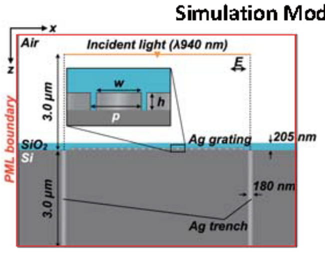

Note: Dimensions are for Case I.

- Full WAVE, DiffractMOD
- 940 nm wavelength, p-polarization
- Ag is selected as grating and DTI metal because Ag has the lowest absorption loss.
- DTI width: 180 nm
- 205 nm-thick protection SiO2 covers Ag grating.
- PML (Perfectly matched layer) surrounds the pixel.

Electric Field Intensity Distributions for Case I and Case II

Case I
$\theta_d(1)$=81°

Case II
$\theta_d(1)$=30°
$\theta_d(2)$=85°

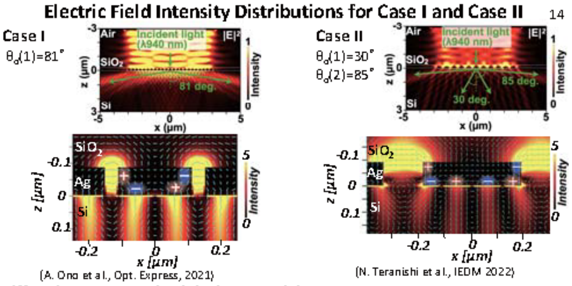

(A. Ono et al., Opt. Express, 2021)
(N. Teranishi et al., IEDM 2022)

- **Diffraction was seen both in Case I and Case II.**
- **Electric multipoles were seen in Ag grating. They generated diffraction light.**

Light Consumption Ratios

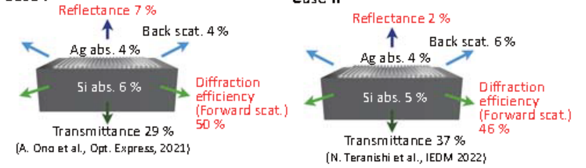

(A. Ono et al., Opt. Express, 2021)
(N. Teranishi et al., IEDM 2022)

- **Both Case I and Case II showed large diffraction efficiency and small reflectance.**
- **Both cases have sufficient potential for NIR absorption improvement.**

Outline

Preferable Reflectance of DTI 17

(N. Teranishi et al., IEDM, 2022)

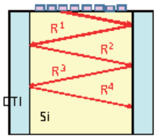

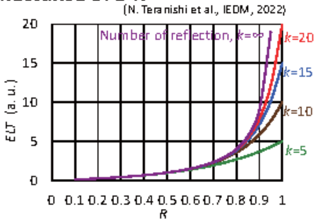

- Reflected by DTI with a loss of 1-R.
- ELT ~ $R(1-R^k)/(1-R)$, (Geometric series)
  ELT: Effective light trace
  R: Reflectance of Si/DTI
  k: Number of reflections

When R > 0.8, ELT rapidly increases with k.
R > 0.8 is preferable.

Reflectance Contours of Normal Incidence to DTI for Combination of n_{DTI} and k_{DTI} 18

(N. Teranishi et al., IEDM, 2022)

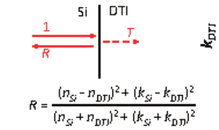

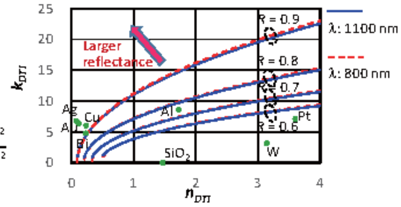

- **When n_{DTI} is smaller and k_{DTI} is larger, Reflectance becomes larger.**
- **Ag, Cu, Au, Bi achieve more than 0.9 reflectance.**

Incidence Angle Dependence of Reflectance 19

(N. Teranishi et al., IEDM, 2022)

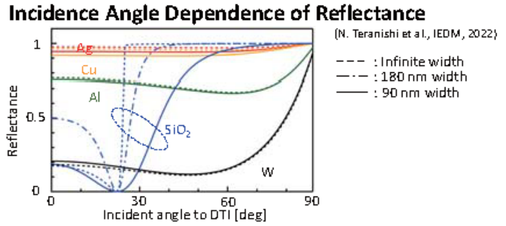

- **SiO2 DTI has low reflectance below the critical angle.**
  Even over critical angle, R ↘ as DTI width ↘ because of evanescent light penetration.
- **Ag and Cu constantly keep R >90 % for all incident angle.**

DTI Width Dependence of R and T 20

(N. Teranishi et al., IEDM, 2022)

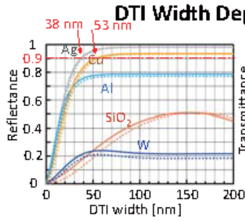

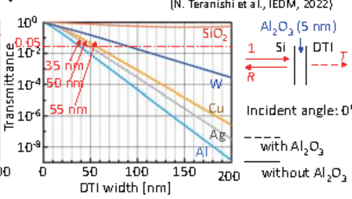

- **Reflectance decreases below 50 nm width even for metal-filled DTI.**
- **For R > 90 %, Ag width > 38 nm, Cu width > 53 nm.**
- **For T < 5 %, Al width > 35 nm, Ag width > 45 nm, Cu width > 50 nm.**
- **DTI width shrinkage is limited even for metal DTI.**
- **Still, Ag, Cu and Al are suitable for high reflective DTI.**

Outline 21

1. **Introduction**
   Application, prior technologies
2. **Plasmonic diffraction under quasi-resonant condition**
   1st-order diffraction, 2nd-order diffraction
3. **Requirements for DTI (deep trench isolation)**
4. **Resonant-chamber-like pixel** ⟵
5. **Conclusions**

More Realistic Pixel Model 22

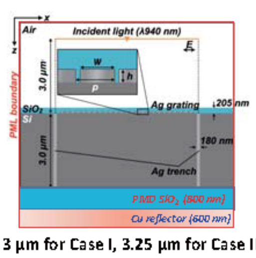

PMD: Pre-metal dielectric

- **Si thickness: 3 µm for Case I, 3.25 µm for Case II.**
- **PMD SiO_2 : 800 nm**
- **First Cu wiring layer is applied for reflector.**

Absorption Enhancement by Plasmonic Diffraction 23

(T. Yoshinaga et al., Opt. Express, 2022)

Case I
Si thickness: 3 µm

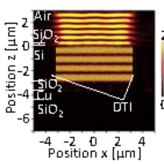

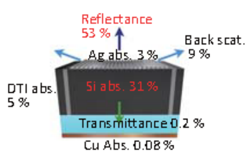

- **Absorptance in Si is increased from 7 % to 31 %.**
- **Resonant patterns are clearly seen in both x and z directions.**
- **Large reflection due to the decoupling of the reversed light.**

Propagation Angle Calculated from Anti-Node Numbers 24

(T. Yoshinaga et al., Opt. Express, 2022)

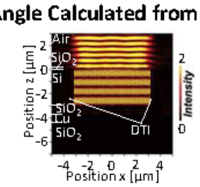

- **Propagation angle, θ is calculated as**

$$\theta = arctan(k_x / k_z) = arctan(m_x l_z / m_z l_x) \approx 80°$$

Wave numbers: kx, kz, Number of anti-nodes: m_x = 48, m_z = 4
Si size: l_x = 6.32 µm, l_z = 3 µm

- **Good agreement with theoretical diffraction angle, 80.6°.**
- **Therefore, incident light was really diffracted to 80°.**

Decoupled Light Outward from Si by Plasmon Resonance

25

(T. Yoshinaga et al., Opt. Express, 2022)

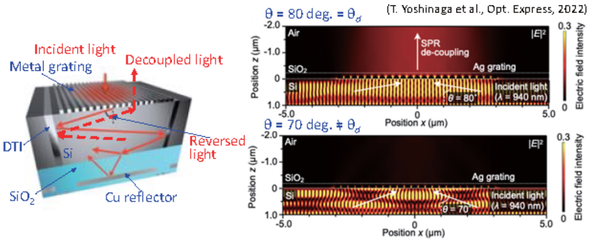

- Total-reflected on Si/SiO_2 interface and propagates at reverse pass.
- Reversed light has the same angle as diffraction angel, θ_d.
- Decoupled light is generated by surface plasmon resonance at metal grating.

Absorption Enhancement by Plasmonic Diffraction

26

(N. Teranishi et al., IEDM, 2022)

Case II

Si thickness: 3.25 μm

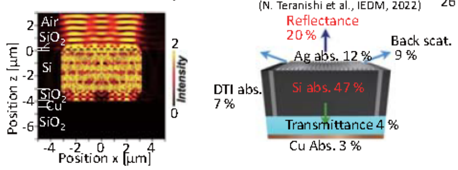

- Resonant patterns are not so clear because there are both 1st and 2nd-order diffractions.
  However, numbers of anti-nodes can be counted.
- Absorptance in Si is much increased to 47 %.
- *R* (Case II) : 20 % << *R*(Case I) : 53 %, because electric field distribution is more complicated, and the decoupling at the grating might be smaller.

Resonant Chamber Effect in Horizontal Direction

27

Case I

without
- bottom SiO_2
- Cu reflector

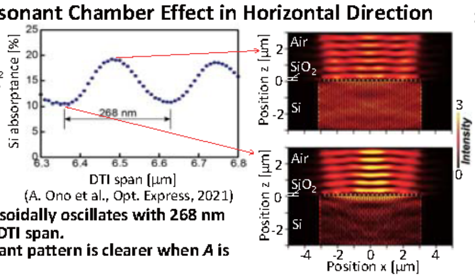

(A. Ono et al., Opt. Express, 2021)

- *A* (Si) sinusoidally oscillates with 268 nm period of DTI span.
- The resonant pattern is clearer when *A* is larger.
- To achieve resonant chamber condition, diffraction angle, θ_d, should be optimized for each pixel size by tuning the grating period.

Resonant Chamber Effect in Vertical Direction

28

(N. Teranishi et al., IEDM, 2022)

Case II

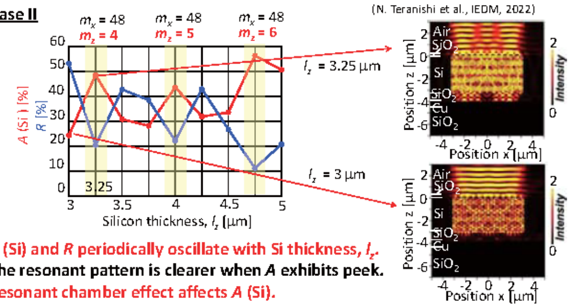

- *A* (Si) and *R* periodically oscillate with Si thickness, l_z.
- The resonant pattern is clearer when *A* exhibits peek.
- Resonant chamber effect affects *A* (Si).

Outline

29

1. Introduction
   Application, prior technologies
2. Plasmonic diffraction under quasi-resonant condition
   1st-order diffraction, 2nd-order diffraction
3. Requirements for for DTI (deep trench isolation)
4. Resonant-chamber-like pixel
5. Conclusions

Conclusions

30

To enhance specific wavelength sensitivity

- Plasmonic diffraction technology under quasi-resonance condition
  - Large diffraction angle, large diffraction efficiency
- High reflective DTI
  - Light confinement in the pixel
  - Ag, Cu, Al
  - DTI width shrinkage
- Resonant chamber effect
  - Should be applied for sensitivity increase.

In simulation,
Absorptance in 3 μm-thick-Si was increased from 7 % to 31 % in Case I.
In Case II, 47 % absorptance is obtained in 3.25 μm-thick Si.